Cortico-Muscular Phase Connectivity During an Isometric Knee Extension Task in People with Early Parkinson's Disease

Nina Omejc, Tomislav Stankovski, Manca Peskar, Miloš Kalc, Paolo Manganotti, Klaus Gramann, Sašo Džeroski, Uros Marusic

***Abstract*— Introduction: Parkinson's disease (PD) is characterized by enhanced beta-band activity (13–30 Hz) in the motor control regions. Simultaneously, cortico-muscular (CM) connectivity in the beta-band during isometric contractions tends to decline with age, in various diseases, and under dual-task conditions. Objective: This study aimed to characterize electroencephalograph (EEG) and electromyograph (EMG) power spectra during a motor task, assess CM phase connectivity, and explore how these measures are modulated by an additional cognitive task. Specifically, we focused on the beta-band to explore the relationship between heightened beta amplitude and reduced beta CM connectivity. Methodology: Early-stage people with PD and age-matched controls performed an isometric knee extension task, a cognitive task, and a combined dual task, while EEG (128ch) and EMG (2x32ch) were recorded. CM phase connectivity was assessed through phase coherence and a phase dynamics model. Results: The EEG power spectrum revealed no cohort differences in the beta-band. EMG also showed no differences up to 80 Hz. However, the combined EEG-EMG analysis uncovered reduced beta phase coherence in people with early PD during the motor task. CM phase coherence exhibited distinct scalp topography and frequency ranges compared to the EEG power spectrum, suggesting different mechanisms for pathological beta increase and CM connectivity. Additionally, phase dynamics modelling indicated stronger directional coupling from the cortex to the active muscle and less prominent phase coupling across people with PD. Despite high inter-individual variability, these metrics may prove useful for personalized assessments, particularly in people with heightened CM connectivity.**

***Index Terms*— Cortico-muscular connectivity, dynamic Bayesian inference, early-stage Parkinson's disease, EEG, EMG, isometric knee extension, motor-cognitive dual tasks, phase coherence, phase dynamics model.**

This work was supported by the European Union's Horizon 2020 research and innovation program under grant agreement No. 952401 (UM). UM also acknowledges financial support from Horizon Europe under grant agreement No. 101120150 as well as from the Slovenian Research Agency (research core funding No. P5-0381). NO and SD also acknowledge financial support of the Slovenian Research Agency via the Research Program Knowledge Technologies (grant P2-0103) and the projects J1-3033, J2-2505, J2-4452, J2-4660, J3-3070, J4-3095, J5-4575, J7-4636, J7-4637, and N2-0236. It was also supported by the EC via the projects ASSAS (grant number 101059682), ELIAS (grant 101120237), INQUIRE (grant 101057499), PARC (grant 101057014), and TAILOR (grant 952215).

Nina Omejc is with the Department of Knowledge Technologies, Jožef Stefan Institute, Ljubljana, Slovenia and with Jožef Stefan International Postgraduate School, Ljubljana, Slovenia (*Corresponsing author*, e-mail: nina.omejc@ijs.si).

Tomislav Stankovski is with the Faculty of Medicine, Ss. Cyril and Methodius University, Skopje, Macedonia and with Department of Physics, Lancaster University, Lancaster, United Kingdom.

Manca Peskar is with the Institute for Kinesiology Research, Science and Research Centre Koper, Slovenia and with the Department of Psychology and Ergonomics, Faculty V: Mechanical Engineering and Transport Systems, Technische Universitat Berlin, Berlin, Germany.

Miloš Kalc is with the Institute for Kinesiology Research, Science and Research Centre Koper, Slovenia and with the Faculty of Medicine, University of Maribor, Maribor, Slovenia.

Paolo Manganotti is with the Clinical Unit of Neurology, Department of Medical, Surgical and Health Sciences, Cattinara Hospital, University of Trieste, Trieste, Italy.

Klaus Gramann is with the Department of Psychology and Ergonomics, Faculty V: Mechanical Engineering and Transport Systems, Technische Universitat Berlin, Berlin, Germany.

Uros Marusic is with the Institute for Kinesiology Research, Science and Research Centre Koper, Slovenia and with the Department of Health Sciences, Alma Mater Europaea University, Maribor, Slovenia.

I. Introduction

PARKINSON'S disease (PD) is a neurodegenerative disorder, characterized by a variety of non-motor symptoms, such as cognitive decline, depression, and sleep disturbance [1], [2], but mainly by motor symptoms like bradykinesia, rigidity, and tremor [3], [4].

The optimal screening tools for early diagnosis of PD are still lacking. The presymptomatic phase of Parkinson's disease pathology in olfactory structures and enteric nerve cell plexuses starts more than a decade before the onset of typical clinical manifestations and diagnosis [5], [6]. Patients are often diagnosed based on motor symptoms during stages III–IV of the Braak model [7], with stage IV representing the most advanced stage of the disease. However, even at these later stages detection remains challenging, with movement-disorder specialists encountering error rates of approximately 20 % [6], [8].

Along with other neurological signs, PD has been characterized by enhanced beta-band in the basal ganglia, cortico-basal ganglia loop and cerebral cortex [9]–[16]. This beta-band over-synchronization of afferents to the motor cortex has been implicated in Parkinsonian bradykinesia and rigidity, which can be treated with pharmacological interventions [17] or deep brain stimulation [18], [19]. Given the observed alterations in brain rhythms, the electroencephalography (EEG) method appears to be a suitable choice for further investigating PD.

Analysis of brain activity using EEG or combined EEG and electromyography (EMG) has not yet been adopted in the diagnostic or examination protocols for PD [6]. Both methods are cost-effective, portable, and capable of recording activity during movement. While EEG is limited in its capacity to measure the activity of subcortical nuclei, some of which the PD directly impacts, cortical regions are also indirectly influenced by activity in these nuclei. The prefrontal association areas, crucial for cognitive functions, are influenced by brainstem nuclei through their efferent connections to the limbic loop centers. Additionally, the degradation of the substantia nigra affects premotor and motor areas by disrupting the nigro-striatal pathway, which in turn affects the cortico-striatal pathway projecting to the motor cortex [3], [7], [20], [21].

A combined measurement of EEG and EMG assesses both central and peripheral neural activities, facilitating the investigation of their functional interactions during movement. It can quantify the synchronization between sensorimotor cortical areas and motor neuron pools, reflecting the cortico-spinal interaction and central drive to skeletal muscles. Various metrics and models have been developed to capture the type, strength, and direction of cortico-muscular (CM) connectivity. One of the well-established connectivity measures is magnitude-squared coherence [22], [23]. Magnitude-squared coherence extends the Pearson correlation coefficient into the frequency domain and is quantified by calculating the normalized cross-spectral density between EEG and EMG signals [22], [24], [25]. Strong CM coherence has been observed in the beta frequency range (13–30 Hz) between different areas of sensorimotor cortex and active peripherical muscles, predominantly during sustained voluntary contractions [23], [26]–[34].

Additionally, in people with PD exhibiting observable resting tremor or myoclonus, significant CM coupling at tremor frequencies (5–8 Hz) has been observed [54]–[56] that was not present in control group or people with PD without observable tremor [57], [58].

While numerous studies have investigated CM connectivity via magnitude-squared coherence, each method has its advantages and limitations. Notable limitations of magnitude-squared coherence include its symmetry, which prohibits the assessment of the direction of connectivity between two signals, and its linearity, which generally fails to capture the complexity of the nonlinear sensorimotor system [59]. Many other connectivity methods have been used to study cortico-cortical connectivity, such as phase-amplitude coupling [19], phase coherence or phase locking value [60]–[62], and autoregressive modelling techniques such as Granger causality, directed transfer function [63], [64] and (nonlinear) partial directed coherence [65]–[67]. Other methods include model-free methods that are based on information theory, such as mutual information, transfer entropy [68]–[70] or (time-frequency) maximal information coefficient [71], [72]. Moreover, various methods for assessing effective connectivity have been explored, where the parameters of preselected models are estimated based on empirical data. Notable examples of these methods are dynamic causal modelling [73] and dynamical Bayesian inference [74]–[76].

In this study, we have chosen to evaluate functional connectivity within the phase domain, because it can directly explore temporal relationships between neural signals [77]. We employ phase coherence and perform phase dynamics modelling using dynamical Bayesian inference.

Magnitude-squared coherence analysis can detect whether two processes exhibit oscillations within the same frequency range, but cannot separate the effects of amplitude and phase [61] or determine whether these oscillations are independent or coupled [62], [78]. In contrast, phase coherence or phase locking value measures the consistency of the phase difference between two signals over time and across frequencies, giving additional insights into the phase coupling or synchrony between signals. This has been proposed as essential for processes such as perceptual binding, long-range synchronization, or control of the excitability in distant neuron groups [61], [79]–[82]. Phase analysis has been already used in examining CM interactions [83]–[85], also using more general multi-spectral phase coherence [86], [87], but we could not find any results for our cohort of people with PD.

Additionally, we aimed to model the CM phase connectivity as a system of coupled phase oscillators following the Kuramoto model [88], [89], inferred via dynamical Bayesian inference [74]–[76]. This method falls under effective connectivity approaches, where a specified model directly explains the causal dynamics [90]. It allows for a detailed definition of the coupling functions between the signals and enables the determination of the coupling direction between EEG and EMG. The phase dynamics model describes a phase oscillator and its rate of phase change, which is governed by the intrinsic frequency. When coupled to other oscillators, the oscillator is also influenced by their phases via coupling functions. By finding the most influential coupling functions, we can characterize the strength and nature of the signal coupling [91], [92]. The simplicity and scalability of the phase dynamics model make it well-suited for capturing the oscillatory activity commonly observed in EEG and EMG signals. The method has been previously applied to modelling cortico-cortical connectivity [93]–[95], but its application to CM connectivity has not yet been explored.

In this study, we aim to explore the CM phase connectivity in people with early-stage PD and age-matched healthy controls during an isometric knee extension task. Specifically, our objectives are to: characterize the EEG and EMG power spectra, as well as CM phase connectivity, with a particular focus on the beta-band; assess how these measures are modulated by the addition of a cognitive task; and evaluate their potential as biomarkers for diagnosis or rehabilitation.

II. Methodology

A. Participants

A total of 22 people with an early diagnosis of PD (Hoehn and Yahr stage I–II) have been recruited in the study, together with 27 age and gender-matched healthy participants. All patients with PD received anti-parkinsonian medications. Motor

performance in all participants was assessed by the Movement Disorder Society Unified Parkinson's Disease Rating Scale (MDS-UPDRS) [96], administered by an experienced neurologist. In the final analysis of this study, data from 15 patients with PD (6 females) and 16 healthy participants (7 females) were included.

TABLE I
DEMOGRAPHIC AND CLINICAL CHARACTERISTICS OF PARTICIPANTS

	People with PD		Controls	
	Mean	SD	Mean	SD
Age (years)	63.8	6.2	63.7	7.2
BMI	25.3	4.1	24.6	7.3
Years of Edu.	11.9	3.6	15.5	3.7
MoCA	27.1	1.6	27.3	1.7
UPDRS III	14.7	6.8	-	-
UPDRS Total	27.5	15.9	-	-

BMI: body-mass index, Edu.: Education, MoCA: Montreal Cognitive Assessment Score, UPDRS: Unified Parkinson's Disease Rating Scale.

Several participants were excluded due to the unavailability of data (some participants did not complete this part of the study), or excessive noise in the collected data. The average and standard deviation of the body-mass index, years of education, the Montreal Cognitive Assessment (MoCA) score, and UPDRS scores are shown in Table I for both cohorts. UPDRS scores are not available for the control cohort.

All participants provided written informed consent prior to the study. The study adhered to the Declaration of Helsinki and received approval from the ethics committee. The study was registered at IRB of Trieste University Hospital - ASUGI, Trieste, Italy (ASUGI protocol number: 106/2021; approved on 20.12.2022) and on ClinicalTrials.Gov under the code NCT05477654.

B. Experiment

The experiment was conducted as part of our clinical trial. For a comprehensive description of the methodology and protocols, please refer to Marusic *et al*. [97]. In this part of the experiment, participants engaged in three tasks (see Fig. 1A): a single task - motor, a single task - cognitive, and a dual task, where they had to perform motor and cognitive tasks simultaneously. The motor task was performed with each leg separately.

The motor task is shown in Fig. 1B. Participants had to perform an isometric knee extension task, which involved a 32-second force tracking session with a trapezoidal pattern (6-second rising phase, 20-second sustained phase, 6-second decline phase). The task was performed with the right and left lower limbs separately. Participants were instructed to actively contract their knee extensors to produce force up to 30% of their maximum voluntary contraction (MVC). A knee extension dynamometer equipped with a force sensor was used to provide feedback to participants. Feedback was shown on the computer screen in front of them, together with the desired force level.

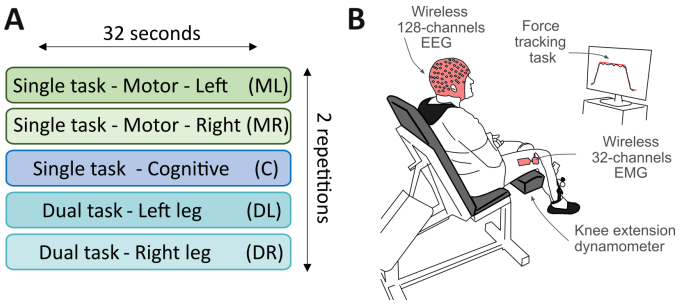

Fig. 1. Overview of Experimental Tasks. Subfigure **A**: Schematic representation of the experimental tasks. Subfigure **B** depicts the motor task, specifically an isometric knee extension task. It was taken and edited with permission from the published study protocol of Marusic *et al*. [97].

In the cognitive task, participants were required to mentally (quietly) perform a serial-3 subtraction task. This task involved subtracting a number 3 from a randomly selected 3-digit number between 300 and 500. They had to do this for 32 seconds and at the end report the number they had reached.

The order of limb usage and task conditions was counterbalanced across participants, with the single task conditions performed before the dual task for each limb. Each of the five conditions was repeated twice.

C. EEG & EMG measurements

EEG activity was recorded with a mobile 128-electrode wireless system (CGX, Cognionics Inc., San Diego, USA), following the 10-5 electrode placement system [98]. We used Ag/AgCl wet electrodes, with a 500 Hz sampling rate, 24 bits of resolution, and no filter settings. The electrode impedance was kept below 20 $k\Omega$ for each channel and balanced across all channels within a 5 $k\Omega$ range. Reference and ground electrodes were placed on the right and left mastoids, respectively.

EMG activity was monitored using two wireless 32-channel probes (MUOVI, OT Bioelettronica S.r.l., Torino, Italy), with electrodes positioned on the bilateral *vastus lateralis* muscles. We used Ag/AgCl wet electrodes, with a 2000 Hz sampling rate, and no filter settings. The electrode, serving as both the reference and ground, was placed on the patella of each knee, with each EMG system having its dedicated electrode. A common digital signal was used to synchronize EMG and EEG data offline.

A schematic overview of the EEG & EMG data analysis pipeline is shown in Fig. 2. The code used to preprocess the data and calculate connectivity measures is available on GitHub at `https://github.com/NinaOmejc/cmcpd.git`. It was written in Matlab (version 2023a, The Math Works, USA), using EEGLAB toolbox [99] for preprocessing, Multiscale Oscillatory Dynamics Analysis software [100] for phase connectivity analysis and custom scripts. To synchronize the EEG and EMG data, the EMG data stream was adjusted from an initial sampling frequency of 2000 Hz to 500 Hz, to match the EEG sampling frequency. The two datasets were aligned using a common trigger. Following this alignment, extensive preprocessing was applied to both the EEG and EMG data.

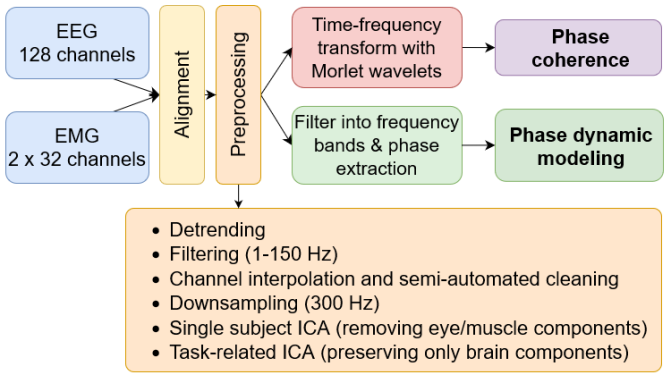

Fig. 2. Analysis diagram, showing the processing workflow of the acquired EEG and EMG signals, including the preprocessing and main connectivity analysis steps.

1) Preprocessing: We first excluded non-task data and removed flat-line EMG electrodes. Next, we removed the trend in the signal by subtracting the moving average calculated over 10-second time windows. The data were then filtered using a high-pass filter with a 1 Hz cut-off frequency and a low-pass filter with a 150 Hz cut-off frequency (Hamming windowed sinc FIR filters) [99]. We employed the Zapline-plus method to remove line noise [101], [102]. EEG electrodes with excessive artefacts were automatically detected using the Clean Rawdata EEGLAB plug-in with subsequent manual inspection. The final set of bad electrodes was interpolated using spherical spline interpolation. On average, we interpolated 24/128 electrodes per data set (SD=10.8). After channel interpolation, another manual inspection was conducted to remove any bad data segments. Subsequently, the EEG data was re-referenced to the average reference, and both EEG and EMG data were downsampled to 300 Hz. Table in Appendix I presents the final amount of clean data, categorized by cohort and task.

As the final two preprocessing steps, two independent component analyses (ICA) were performed on EEG data, using *runica (Infomax)* algorithm in EEGLAB toolbox. In the first ICA analysis, data from each participant (over all tasks) were concatenated to facilitate the removal of ocular, muscular, and cardiac independent components (ICs), specific to each individual. ICs components were selected with the help of ICLabel plug-in [103], dipole position [104]. On average, 32 ICs were removed (SD = 9) per participant. Remained ICs were projected back to the scalp electrodes.

In the second ICA analysis step, we merged all EEG data from a single task across all participants to identify task-specific brain components. With the same approach as for the first ICA step, we manually retained the top 20 ICs across all datasets. Again, kept ICs were projected back to the electrodes.

Importantly to note, we did not rectify EMG data to not additionally modify the frequency spectrum and the phase of the signals [105]–[107]. However, for further analysis, we reduced the data dimensionality by averaging all 32 EMG time series for each leg. Beforehand, we confirmed that prior averaging had a minimal impact on the results. This is further demonstrated in Appendix II.

2) Continuous wavelet transform: To calculate phase coherence, we first had to transform the continuous, cleaned EEG and EMG data into the time-frequency domain. We calculated continuous wavelet transform, $\mathcal{W}_x(\omega, t)$, of a signal $x(t)$ at angular frequency ω and time t as in [94], [100]:

$$\mathcal{W}_x(\omega, t) = \int_0^\infty \psi(\omega(u-t))x(u)\omega \, du, \tag{1}$$

$$\psi(u) = \frac{1}{2\pi}(e^{i2\pi f_0 u} - e^{\frac{(2\pi f_0)^2}{2}})e^{-\frac{u^2}{2}}. \tag{2}$$

We employed a Morlet wavelet $\psi(u)$ with a central frequency parameter $f_0 = 1$, 30 voices per octave, $\int \psi(t)dt = 0$. Symbol i is the imaginary unit. The frequency boundaries were 4-90 Hz. The wavelet power of the EEG was computed as $|\mathcal{W}_x(\omega, t)|^2$ for each scalp electrode whereas the wavelet power of the EMG was determined from the averaged time series across all 32 electrodes for each leg.

Due to the limited number of trial repetitions, we averaged the wavelet power over time. To further conduct group analysis, we performed a z-transformation on the EEG wavelet power, across all electrodes and frequencies. Such standardization procedure allowed for a more equitable averaging across subjects by ensuring that the data were on a common scale. As such, the analysis did not focus on absolute power values but rather on the relative strength of power at specific electrodes compared to others on the scalp, and at specific frequencies compared to other frequencies. Full details on z-transform are described in Appendix III.

After standardization, we simplified the results by averaging the data from the left and right muscle contractions. This reduction transformed the initial five conditions (see Fig. 1A) into three consolidated task categories: single motor task, dual task, and single cognitive task. Before combining the data, we examined the data for any lateral differences above the central brain region, which were not observed. The lack of laterality, which is typically prominent in motor tasks, is attributed to the specific motor task selected. The neuronal population responsible for knee extension movement is located medially within the motor cortex gyri [108], with regions from both hemispheres positioned so closely that EEG could not distinguish positional differences.

Finally, to conduct statistical comparisons on our 2-by-3 design with non-normally distributed values, we computed p-values using the Scheirer–Ray–Hare (SRH) test [109] at each frequency. To account for multiple comparisons, we applied the false discovery rate (FDR) correction [110]. Differences were considered significant if p-values were below the significance level $\alpha = 0.05$. We examined differences in the main factors of task and cohort, as well as their interaction effect. We further assessed the pairwise significance using the non-parametric Wilcoxon test [112].

3) Phase coherence calculation: Phase coherence or phase locking value [60], [111] is a statistical method that computes how consistent or stable the phase difference between the two signals is over time, regardless of whether the actual phase difference is zero [61], [62]. Phase coherence $\mathcal{PC}(\omega)$

was calculated pairwise between each EEG electrode and the averaged EMG of each leg, following Eq. 3.

$$\mathcal{PC}(\omega) = \left| \frac{1}{T} \sum_{t=1}^{T} e^{i(\theta_{eeg}(\omega,t) - \theta_{emg}(\omega,t))} \right|, \tag{3}$$

where $\theta_x(\omega, t)$ is the angle of $\mathcal{W}_x(\omega, t)$, T represents the number of time points and ω the angular frequency. Phase coherence was calculated at each time point t but was then averaged over both trials.

We conducted z-transformation and statistical analyses over frequencies in the same way as analyses for wavelet power results. Additionally, we extracted individual maximum low-beta values and statistically compared the distributions between cohorts and tasks, using a pairwise non-parametric Wilcoxon rank-sum test [112].

Besides the z-transformation, which provides a relative view of the phase coherence distributions and facilitates comparison between cohorts, an alternative method for assessing significance involves generating randomized surrogates of the original signals [113]. To create the surrogate time series, we used the cycle phase permutation surrogates [113], which are designed for phase dynamics. We calculated 100 surrogate time series per participant. When presenting non-standardized phase coherence, we also display the surrogate distributions by plotting their mean and standard deviation.

4) Phase dynamics modelling: We modelled phase connectivity between two signals as coupled phase oscillators based on the Kuramoto model [88], [89], which is well-suited for biological signals due to their inherent rhythmicity [91]. The phase dynamics of two coupled oscillators i and j are described in Eq. 4:

$$\begin{aligned} \dot{\theta}_i &= \omega_i + q_i(\theta_i, \theta_j) + \xi_i, \\ \dot{\theta}_j &= \omega_j + q_j(\theta_i, \theta_j) + \xi_j. \end{aligned} \tag{4}$$

A pair of differential equations tell how the phase θ_i of the signal i changes with its intrinsic frequency ω_i and by the influences from other oscillators, as described by $q_i(\theta_i, \theta_j)$. The term ξ corresponds to the white noise. A similar relationship applies reciprocally to oscillator j. An extended version of the phase dynamics model with 24 coupling terms inside the coupling function $q_i(\theta_i, \theta_j)$, that was fitted to the data, is shown in Appendix IV. We first applied a 4th-order Butterworth filter to the data, selecting the narrow low beta-band range (12.5–20 Hz). A filtfilt procedure was used to eliminate zero-lag disturbances. We then extracted the instantaneous protophase signals using the Hilbert transform and converted them to phase signals via the protophase-to-phase transformation [114]. We then fitted the extended phase dynamics model pairwise between the phase signals of each EEG electrode on the scalp and the average EMG of each leg.

We applied dynamical Bayesian inference to reconstruct the matrix of coupling coefficients and noise strength, fully characterizing the oscillator coupling [75], [76], [94]. Further details of the inference method can be found in Appendix V.

The model was inferred over the 3-second time windows, with a 50 % overlap. The main outcome of dynamical Bayesian inference analysis is a $N \times K$ matrix, where $K = 50$ represents the inferred coefficients c_k, which include the oscillator's intrinsic frequency and the coupling terms. Each of the two equations contributes 25 coefficients, which are calculated for all N time windows. Due to the initial convergence of the prior, we removed the results of the first 5 windows from the final analysis.

After the parameter inference, we aimed to identify the most significant coupling terms in the model. To do this, we calculated the average absolute values of each of the 24 coefficients across all participants, and compared it to distributions of surrogate absolute parameter values. The surrogates were calculated as already explained in the previous subsection for phase coherence calculation. Coupling terms with absolute values above the surrogate threshold (average + 2 SD) over all categories were considered dominant coupling terms.

To quantify the coupling strength between two oscillators i and j, we calculated Euclidean norm of the dominant coupling terms: $\sigma^{(i,j)} = \sqrt{\sum_{m \in M} (c_m^{(i,j)})^2}$, where M denotes the set of indices corresponding to the dominant coupling terms.

In addition to investigating the coupling strength, we aimed to compare the individual shapes and variances of the coupling functions. To accomplish this, we calculated the similarity index [115], which represents the correlation coefficient between the coupling functions: $\rho = \frac{\langle \tilde{q_1}\, \tilde{q_2} \rangle}{||q_1||\, ||q_2||}$, where $\langle \cdot \rangle$ denotes spatial averaging over the 2D domain, $\tilde{q}$ denotes $q - \langle q \rangle$, and $||q|| = \langle qq \rangle^{\frac{1}{2}}$. There are also conditions that $0 <= \phi_1$, and $\phi_2 <= 2\pi$. We calculated the similarity indices between the median coupling functions of each cohort and the dominant coupling function, as well as among the median coupling functions of each cohort.

III. Results

We conducted an experiment involving an isometric knee extension task, with and without an additional cognitive component. It included 16 people with Parkinson's disease (PD) and 15 matched healthy controls (HC). Following data collection and preprocessing, we computed power frequency spectra and cortico-muscular (CM) phase coherence and modelled the CM data as coupled phase oscillators by inferring the phase dynamics model using dynamical Bayesian inference. The results are presented in the same sequence.

A. Wavelet power frequency spectra

First, we show the results of EEG wavelet time-frequency transformation. Fig. 3 shows the topographical distribution of standardized EEG power for three frequency bands: alpha (7–12 Hz), beta low (12.5–20 Hz), beta high (20.5–30 Hz), whereas the topographical distributions of power in gamma low (30.5–48 Hz) and gamma high (52–90 Hz) can be seen in Appendix VI.

An initial observation is that each task exhibits a distinct topographical power distribution that is consistent across both cohorts and, to some extent, across frequency bands. During the motor task (first row in Fig. 3), the highest relative power was observed over the fronto-central region, (at enlarged electrodes Fz, FCz, FC1, and FC2). High rhythmic activity in

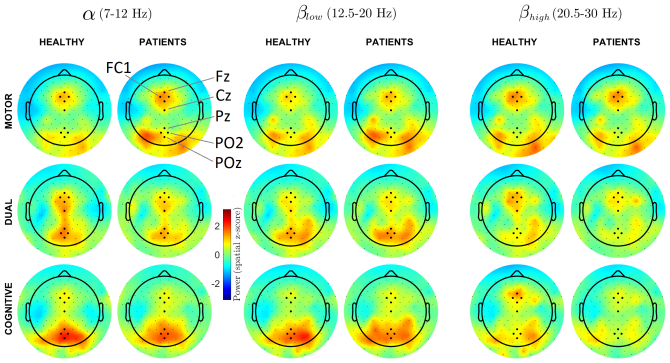

Fig. 3. Topological distribution of relative EEG wavelet power. EEG power distribution is shown across tasks (motor, dual, cognitive), frequency bands (alpha, beta low, and beta high), and cohorts (people with PD and healthy controls) over the scalp electrodes. The power values were standardized across electrodes and frequencies and averaged across the trial length, trials, and participants within the cohort. The black dots on the plots correspond to electrode positions. Some dots over the strongest activity regions are enlarged for easier comparison. The five groups of enlarged electrodes are: fronto-central cluster (FCz, Fz, FC1, FC2), central electrode Cz and parieto-occipital cluster (Pz, POz, PO1, PO2). Note that the values are z-scored, making them relative to each other, and, consequently, include negative values.

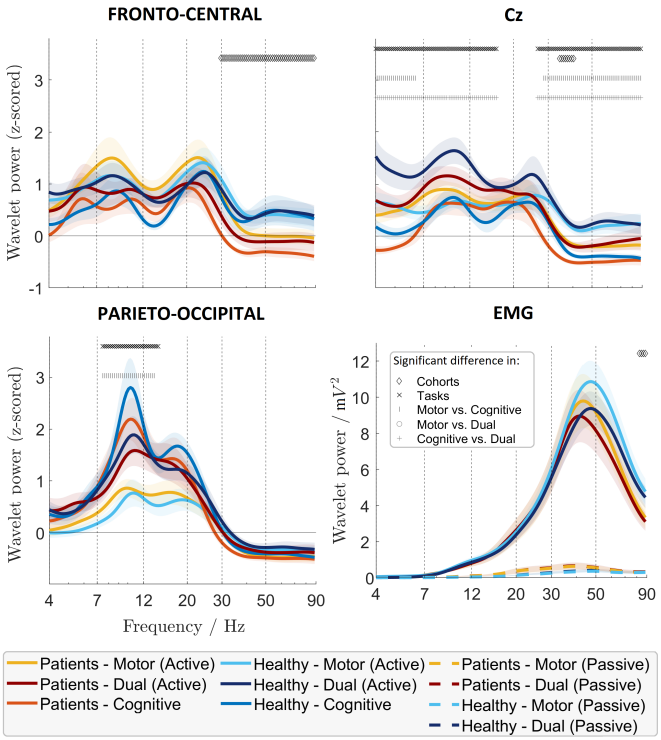

Fig. 4. Wavelet power spectra of EEG & EMG signals, categorized by region, cohort, and task. The subfigures present spatially standardized power spectra for fronto-central (Fz, FCz, FC1, FC2), central (Cz), and parieto-occipital (Pz, POz, PO1, PO2) brain regions, as indicated by the titles above subfigures. The subfigure titled EMG shows EMG wavelet power spectra, categorized by leg, cohort, and task. Colours represent cohort-task groups as indicated in the legend below the figure. Solid lines indicate the mean power of the active leg, dashed lines indicate the mean power of the passive leg, and shaded areas represent the +/- one standard error (SE). Significant differences between tasks and cohorts at particular frequencies are marked at the top of the plots with dark markers, as depicted by the legend in the subfigure titled EMG. Frequency is plotted on a logarithmic scale. Note that the values are z-scored, making them relative to each other, and, consequently, include negative values.

this region spanned a range of frequencies, from alpha to low gamma. In the dual task, the fronto-central region continued to show high relative power (second row in Fig. 3) but it was generally lower compared to the single motor task. During the cognitive task (third row in Fig. 3), activity over sensorimotor areas decreased even further, and only relatively strong high beta power was observed in a healthy cohort.

Conversely, the medial parieto-occipital region (enlarged electrodes Pz, POz, PO1, and PO2) exhibited the highest activation during the cognitive task, particularly in the alpha and low beta-bands. This strong rhythmic activity was less pronounced during the dual task and even less so during the single motor task.

To further quantify the differences, we looked at frequency spectra at the three regions with the highest activity: fronto-central cluster, central Cz electrode, and parieto-occipital cluster, and plotted them in Fig. 4. The frequency spectra align with the topographical plots, illustrating distinct patterns of activity across different brain regions regardless of the cohort. In the fronto-central region, the strongest power was observed in alpha and high beta frequency ranges. It was the strongest during the motor task, followed by the dual task, and finally the cognitive task. In the central region, the peak power was again observed in alpha and high beta regions. It was the strongest in the dual task, followed by the motor task, and lastly in the cognitive task. Conversely, in the parieto-occipital region, the strongest peak power was in the alpha frequency range. The cognitive task induced the strongest rhythmic activity, followed by the dual task and the motor task. However, it is important to note that not all observed qualitative differences were statistically significant.

Statistically significant task-related differences were observed only in the central Cz electrode and parieto-occipital regions. At Cz, power during the cognitive task was significantly lower when compared to the single motor task for frequencies between 4-6 Hz (mean p-value = 0.01) and 29-90 Hz (mean p-value = 0.007) and when compared to the dual task, power was lower for frequencies between 4–17 Hz (mean p-value = 0.003) and 26-90 Hz (mean p-value = 0.006). In the parieto-occipital region, we observed statistically significant differences between motor and cognitive tasks during 7–14 Hz (mean p-value = 0.009).

Statistically significant differences between cohorts were observed exclusively within the gamma frequency ranges. These differences were significant in the fronto-central cluster for all frequencies exceeding 30 Hz (mean p-value = 0.005) and at the Cz electrode, specifically within the narrow frequency range of 35 to 40 Hz (mean p-value = 0.04). People with PD exhibited consistently lower relative power compared to healthy controls. Although we observed high beta power peaks, these did not show statistically significant differences between the cohorts.

The EMG frequency spectra for muscle contractions at 40 % MCV peaks between 40-50 Hz (Fig. 4, subfigure

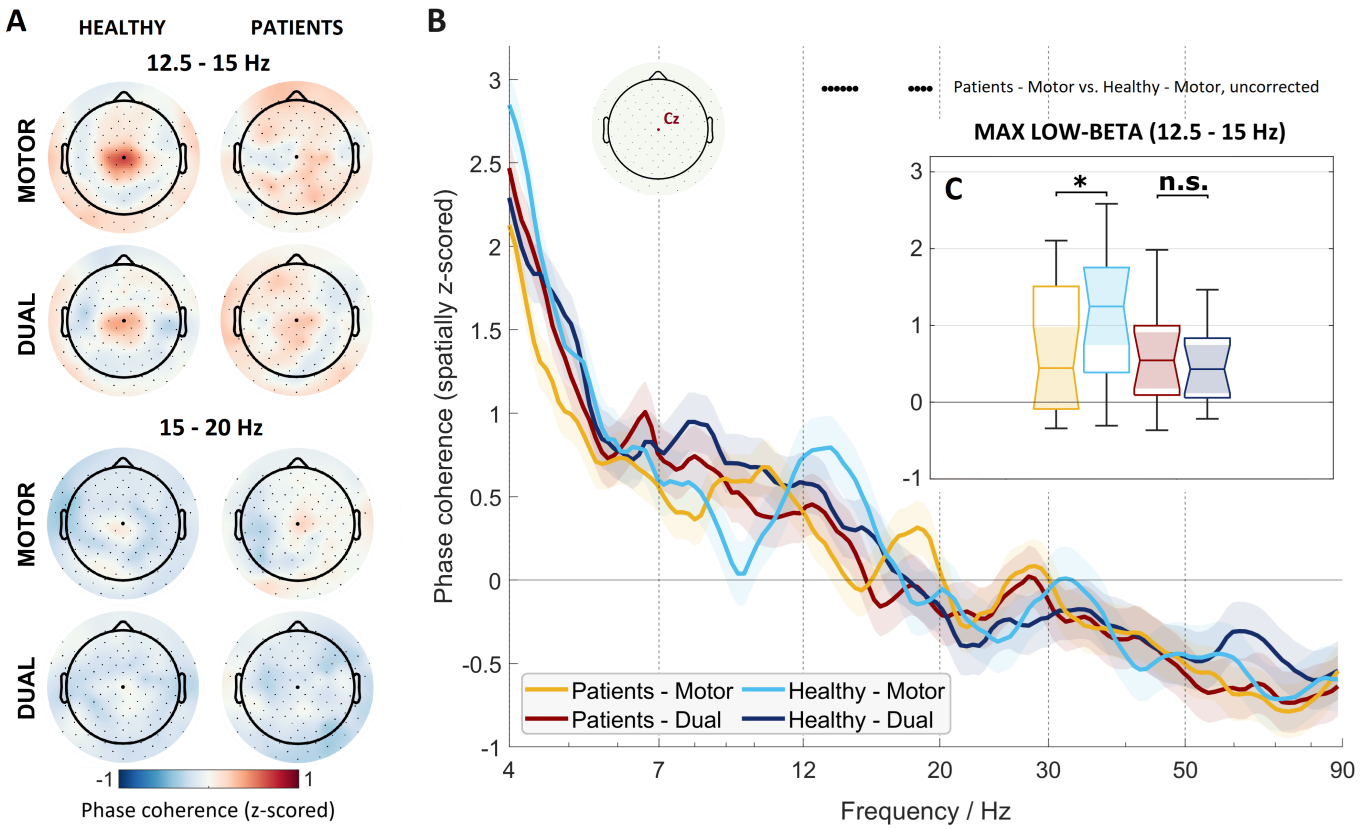

Fig. 5. CM phase coherence results topographically and at Cz electrode. **A:** Topographical plots show the lower beta phase coherence between the respective scalp electrode and the EMG signal of the active leg. The upper four plots depict phase coherence at 12.5–15 Hz across both cohorts (people with PD / healthy) and tasks (motor / dual). The lower four plots represent CM phase coherence for the same categories but at a 15–20 Hz frequency range. The enlarged dot corresponds to the location of the Cz electrode. **B:** CM phase coherence of active muscle at Cz electrode across all frequencies (x-axis). Solid lines represent the mean, while the shaded areas represent the +/- 1 SE. Significant differences between cohorts for the motor task are marked with black dots at the top of the plots but note that these p-values were uncorrected for multiple comparisons. **C:** The inset plot shows distributions of maximum low-beta values between 12.5–15 Hz for the four groups, as colour-coded by the legend. The abbreviation n.s. indicates a non-significant difference, while the star denotes $p < 0.05$. Note that the values are z-scored, making them relative to each other, and, consequently, include negative values. Positive phase coherence indicates that the phase coherence for a specific frequency band and electrode position exceeded the average, while negative phase coherence denotes that it was below the average.

EMG). While we observe higher power during the single motor task compared to the dual task, the differences are not statistically significant. Similarly, although the healthy cohort demonstrates higher peak power in both tasks, we do not find statistically significant differences in the peak EMG power spectra. However, we do observe significant differences at frequencies above 82 Hz (mean p-value = 0.04).

B. Cortico-muscular phase coherence

We first present the topographical plots of relative (standardized) CM phase coherence between the EEG electrodes and the averaged EMG for the active muscle in Fig. 5A. The plots show the distribution of CM phase coherence for the lower beta-band, separated into frequency ranges of 12.5–15 Hz and 15–20 Hz. We focused on the beta-band, as has been previously documented as an important frequency range for CM coherence and isometric contraction in general (see Introduction). The topographical plots of other frequency bands are in Appendix VIII. Collectively, these plots revealed that the central region around the Cz electrode exhibits the relatively strongest phase coherence with the EMG signal of the active muscle. Based on this observation, we further analyzed the phase coherence at the Cz electrode. Appendix II presents example phase coherence results for two individual participants, while the group analysis is shown in the B and C parts of Fig. 5.

In Fig. 5B, we show CM phase coherence over the frequency spectrum for all four cohort-task groups. By comparing phase coherence values between them, none of the significance levels survived the multiple comparisons correction. However, uncorrected pairwise significant differences between cohorts found in frequency ranges 13–15 Hz and 18–19 Hz (see black dots on top of Fig. 5B) were used as guiding ranges to extract maximum CM phase coherence values. The reason we decided to also check maximum values over the range, instead of only looking at differences in particular frequencies, is that there is generally a high variability in peak coherence (e.g. see [27], [36], [46], [117], [120]). This approach thus better accounts for inter-individual differences, as different subjects normally have peak CM phase coherence at different peak frequencies.

We depicted the distributions of maximum coherence levels for each cohort-task group with boxplots in inset Fig. 5C. We found significant differences in the main factor task ($p =$

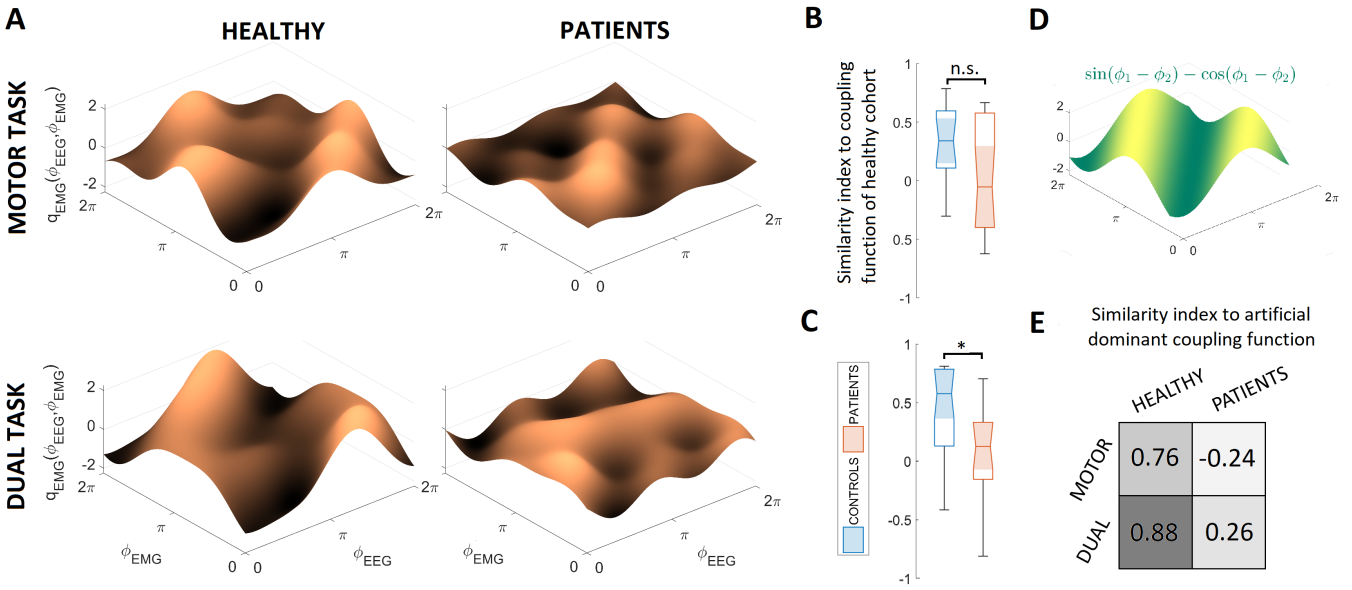

Fig. 6. Inferred coupling functions from the phase dynamics model from EEG Cz electrode to average EMG of the active muscle. **A:** Median coupling functions, grouped by cohort and task. **B:** Boxplots show the distributions of similarity indices within cohorts, for the motor task and **C:** for the dual task. Distributions are also compared between cohorts, with a star indicating $p < 0.05$ and n.s. indicating no significant differences. **D:** Depiction of coupling function with the two dominating terms. **E:** Matrix showing similarity indices between the dominant coupling function and the median coupling function for each group.

0.031) and significant pairwise differences between people with PD and healthy controls during the single motor task ($p = 0.031$), in the frequency range of 12.5–15 Hz. No such significant pairwise differences were observed during the dual task ($p = 0.74$). Additionally, we did not find any significant differences between maximum CM phase coherence in the frequency range of 15–20 Hz (not shown). Given that z-transformation is not commonly employed in this field, we also provide the non-transformed values of phase coherence in Appendix IX, where the median was chosen as an aggregating function. The findings are consistent with those obtained after z-transformation. Additionally, in Appendix IX we also present the results for the CM phase coherence between Cz EEG and the EMG of the passive muscle, where, as expected, there were no significant differences between the cohorts or tasks.

C. Phase dynamics modelling

After obtaining a strong beta-band CM phase coherence at the Cz electrode, we modelled the same interaction using the phase dynamics model. In this subsection, we present the inferred coupling functions for the four task-cohort groups, and compare their shapes and coupling strengths.

Inferred coupling functions between EEG Cz electrode and average EMG of the active muscle are graphically presented in Fig. 6A.

The coupling function plots are derived by graphing all 24 coupling functions over the period from 0 to 2π, with each function weighted according to the inferred coefficients. If there are no dominant terms, the landscapes appear unstructured; conversely, the plots exhibit discernible structure when dominant terms are present. By visually comparing the median landscapes between the cohorts, a diagonal structure is evident in the healthy cohort during both tasks, which is absent in the patient cohort. To quantitatively compare the coupling functions, we used a similarity index. The results are for the active muscle presented in Fig. 6B for the motor task and in Fig. 6C for the dual task. The analysis revealed that the median similarity index within the healthy cohort for the motor task is 0.34 and 0.58 for the dual task. On the other hand, between the median healthy cohort and individual patients with PD, we observe notably lower median similarity indices (motor task: -0.05, dual task: 0.13). In the motor task, no significant differences between the cohorts were observed. However, in the dual task, the differences between cohorts were statistically significant ($p = 0.046$), suggesting that the coupling functions of people with PD differ significantly from those of the healthy cohort.

Furthermore, inferred models for the active muscle are shown in Appendix X. The inferred intrinsic frequencies of the phase oscillators range between 13.6 and 15 Hz, aligning well with the peak levels of the low-beta CM phase coherence in the healthy cohort. Notably, the models presented only include dominant coupling functions. To identify them, we compared the absolute magnitudes of inferred coefficients to the surrogate distribution, as shown in Appendix X. We found two significant dominant coupling terms in the connectivity to the active muscle: $p_{11}\sin(\theta_{emg} - \theta_{eeg})$ and $p_{12}\cos(\theta_{emg} - \theta_{eeg})$, which are plotted in Fig. 6D. The similarity indices between them and the coupling functions of individual groups are shown in Fig. 6E. They are higher in the healthy cohort for both motor ($\rho = 0.76$) and dual tasks ($\rho = 0.88$). In people with PD, the similarity indices are markedly lower, with $\rho = -0.24$ in the motor and $\rho = 0.26$ in the dual task.

Finally, the coupling strength was quantified by calculating the norm of the two coefficients corresponding to the dominant coupling terms. The distributions of coupling strengths for both directions, tasks, and cohorts are shown in Fig. 7. We observed that the strength of coupling from EEG to EMG was significantly greater than in the reverse direction ($p = 1.6 \times 10^{-5}$), which is to be expected. Further analysis of coupling strengths in the active muscle between cohorts and tasks using the SRH test revealed that the main effect of the task was not significant ($p = 0.83$), while the main effect of the cohort approached significance ($p = 0.056$). No significant differences were found when comparing the cohorts for each task individually (motor task: $p = 0.34$, dual task: $p = 0.10$). However, pairwise comparisons of coupling strength between cohorts, irrespective of the task, showed a significant difference ($p = 0.0494$), indicating stronger coupling in the healthy cohort.

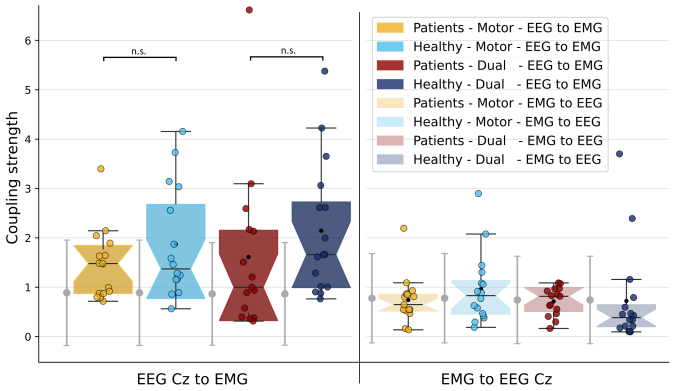

Fig. 7. Phase coupling strength between the Cz EEG electrode and the active muscle. The coupling strength is grouped by the coupling direction (left and right side of the plot) and by cohort and task direction as colour-coded by the legend. Black circles in each distribution correspond to the average value, while the coloured dots correspond to the individual participant's values. Grey error bars represent the surrogate average +/- 2 SD.

The phase modelling results between Cz EEG and the EMG of the active muscle, as presented here, are also shown for the passive muscle in Appendix XI. In summary, no statistically significant dominant coupling functions were observed in either group, and no significant differences were found between the cohorts.

IV. Discussion

This study investigated cortico-muscular (CM) phase connectivity in early-stage people with Parkinson's disease (PD) and age-matched healthy controls during three tasks: the motor task (isometric knee extension task), the cognitive task (silent serial -3 subtraction task) and the dual task, where both motor and cognitive tasks had to be performed simultaneously. We calculated phase coherence and inferred the phase dynamics model. The findings of our study are point by point discussed below.

Topographical task-dependent variations in wavelet power spectra outweigh the cohort differences. Our study demonstrates that distinct patterns of rhythmic brain activity emerged across cortical regions under the three task conditions. While these patterns in power spectra were not consistently significant across the entire frequency range, the general pattern remained observable, particularly in the lower frequency ranges up to 20 Hz. In the fronto-central areas, the wavelet power was the lowest during the cognitive task, characterized by minimal motor involvement, and the highest during the motor task, where focused motor actions dominated the participant's attention. During the dual task where participants engaged in both motor and cognitive activities simultaneously, power levels were at an intermediate level. An inverse trend occurred in parieto-occipital region, where the power up to 20 Hz peaked during the cognitive task, indicating increased cognitive demands. Notably, this region encompasses the intraparietal sulcus (IPS), a critical area involved in arithmetic processing, and number comparison, such as subtraction [121]. These observations align with the dual-task interference concept, which attempts to explain how neural resources are dynamically allocated across cortical regions during multitasking [122]–[125].

People with early PD on medications did not show enhanced power in beta-band. While we did observe the highest peak in the beta-band power (20–30 Hz) in the fronto-central regions during the motor task, it was not significantly higher in comparison to age-matched controls. The absence of elevated power in beta-band, a phenomenon previously reported in people with PD [9]–[15], aligns with the characteristics of our cohort, who are receiving medication [17], and are in the early stages of the disease experiencing minimal motor impairment.

EMG power spectrum up to 80 Hz shows no significant variations by task or cohort. Analysis of the EMG power spectra revealed that the healthy cohort exhibited slightly stronger higher frequency activity in the active muscle for both the single motor and the dual task. However, these differences were not statistically significant until frequencies exceeded 80 Hz, a range that is generally less relevant for combined EEG-EMG analysis. Additionally, in people with PD, no resting tremor was observed, which is commonly associated with increased power in the lower frequency range (around 3–6 Hz, [126]). This absence can be attributed to the fact that patients were in the early stage of the disease, where tremor symptoms were minimal or absent, as well as to the effects of medications. Furthermore, resting tremors are typically lower in lower limbs and suppressed during voluntary motor activity.

The scalp topography of CM phase coherence differs from the topography of the power spectrum during motor tasks. Phase coherence analysis of the motor tasks revealed that the highest phase coherence in the sensorimotor region occurred above the Cz electrode, almost across the entire frequency spectrum (4–90 Hz). Surprisingly, that region does not overlap with the region of the highest wavelet power during movement, which is the fronto-central region. To try to understand this, we found two studies with relevant topographical results to compare with [127], [128], Both studies suggest that there may be greater similarities between the topographical patterns of phase and magnitude CM coherence than between

phase coherence and wavelet power. This implies that wavelet power and phase coherence may reflect different aspects of neural activity. While wavelet power might indicate intense processing that occurs independently of muscle connectivity, phase coherence directly reflects the synchronization between motor output in the central motor cortex and muscle activity, as measured by EMG. These results could also be related to seemingly contradictory phenomena: on one hand, beta-band desynchronization is expected in motor areas during movement preparation and execution [129], which is disinhibited in people with PD and elevated beta-band power is observed. On the other hand, high beta-band coherence between EEG and EMG is typically observed before and during movement [23], [26], [27], [31], [34]. In our study, we observed that both phenomena may exhibit distinct topographies and frequency ranges within the beta-band.

Early-stage PD cohort on medication showed differences in CM phase coherence in the lower beta-band (12.5–15 Hz) during the single motor task. We found differences in CM phase coherence already in patients with early-stage PD, who are on anti-parkinsonian medications, which has not been observed previously [13], [130]. The differences were observed in the lower beta-band, specifically between the 12.5 and 15 Hz frequency range, where the healthy cohort showed elevated CM phase coherence, which was not observed in people with PD. The difference, although significant, was not substantial. This could be attributed to high variability between participants and the fact that the control group were elderly participants, who typically also exhibit reduced connectivity due to age-related factors [39]–[42], [130], potentially influencing the observed difference in phase coherence as well.

Elevated phase coherence was observed only in the healthy cohort during the single motor task, but not during the dual task, which included a cognitive component. The addition of cognitive tasks requires divided attention, which can impair motor performance, particularly in elderly adults and individuals with movement disorders [131], [132]. Previous research has also shown a reduction in beta-band CM magnitude-squared coherence during dual-task conditions [133], [134]. This reduction has been attributed to the hypothesis that beta-band synchronization in the motor cortex requires focused attention, and decreased attention impairs motor neuron recruitment, a mechanism thought to be underlying the cortical beta-band oscillations [133], [135]–[141].

Modelling phase coupling with the phase dynamics model revealed directional asymmetry, showing significantly stronger phase coupling strength from the Cz electrode to the active muscle than vice versa. Despite using different methodologies and examining different muscle groups, our finding aligns with previous studies that employed partially directed coherence [142] and Granger causality [81].

The dominant coupling terms in the phase dynamics model were more pronounced in the healthy than in the patient cohort. We identified two dominant coupling terms that were particularly strong in connectivity to the active muscle: $p_{11}\sin(\theta_{emg}-\theta_{eeg})$ and $p_{12}\cos(\theta_{emg}-\theta_{eeg})$. They represent the sine and cosine components of the phase difference between the EMG and EEG, effectively capturing the phase-locking behaviour and reflecting the coupling between cortical (EEG) and muscular (EMG) oscillatory activity. The diagonal structure of the coupling function suggests that the coupling is determined by the phase difference between the two oscillators [143]. When the coupling function is positive, the influenced oscillator accelerates and vice versa when negative. Such mechanisms are the basis for synchronization phenomena between the oscillators. As a side note, the fact that the inferred dominant terms include phase difference information supports the use of phase coherence measure as a metric of constant phase difference.

Dominant coupling functions showed qualitatively stronger coupling strength in the healthy cohort compared to the patient cohort, although only marginally significant when the task factor was disregarded. We also observed high variability among participants. Notably, the coupling strength was stronger during the dual task than the single motor task, which is in contrast with the results obtained from phase coherence calculations and something we have to yet better understand.

Neurophysiological markers show limited robustness for clinical diagnosis of PD. With this study, we sought to evaluate the potential of CM connectivity measures as neurophysiological markers for clinical practice. Although we did not directly assess this by employing classification models, our observations show significant inter-subject variability. This suggests that these markers may not be robust or reliable enough for general disease classification. However, they could still be valuable for assessing individual improvements in rehabilitation, especially in people exhibiting strong CM phase connectivity.

Limitations of the study. It is important to acknowledge several limitations of the study. The primary limitation is the low number of trials done by each participant. As the CM connectivity measures are already inherently variable and have high individual differences [36], [46], [117], [120], [144], this even further increased the variance and constrained the assessment of phase connectivity in time. Additionally, we believe this limitation reduced the study's statistical power, preventing some significant differences from surviving correction for multiple comparisons.

Moreover, the study did not account for the delay between EEG and EMG phases when calculating phase coherence or fitting the phase dynamics model. Whereas some studies incorporate delay into the model ([118], [119]) or calculate the delay to assess connectivity direction (e.g. [22]), others do not (e.g. [94]). In our case, we we assume the delay is constant, which implies that the phase difference remains stable and should not substantially affect the results. However, this assumption could have introduced a potential source of error.

Lastly, our analysis remained at the surface level of both the scalp and muscle. For greater spatial accuracy, it would be more appropriate to directly analyze the ICs' time series. A similar decomposition could be applied to motor units within the muscle. However, at this initial stage, we chose to remain at the surface level to also explore the potential for clinical applications, which are more straightforward to implement when source analysis is not required.

REFERENCES

[1] E. Tolosa, C. Gaig, J. Santamaría, and Y. Compta, "Diagnosis and the premotor phase of Parkinson disease," *Neurology*, vol. 72, no. 7, Suppl., pp. S12–S20, Feb. 17 2009. DOI: 10.1212/WNL.0b013e318198db11

[2] J. C. Greenland, C. H. Williams-Gray, and R. A. Barker, "The clinical heterogeneity of Parkinson's disease and its therapeutic implications," *Eur. J. Neurosci.*, vol. 49, no. 3, pp. 328–338, Feb. 2019. DOI: 10.1111/ejn.14094

[3] H. Braak, U. Rüb, D. Sandmann-Keil, W. P. Gai, R. A. de Vos, E. N. Jansen Steur, et al., "Parkinson's disease: Affection of brain stem nuclei controlling premotor and motor neurons of the somatomotor system," *Acta Neuropathol.*, vol. 99, no. 5, pp. 489–495, May 2000. DOI: 10.1007/s004010051150

[4] Q. Wang, L. Meng, J. Pang, X. Zhu, and D. Ming, "Characterization of EEG data revealing relationships with cognitive and motor symptoms in parkinson's disease: A systematic review," *Front. Aging Neurosci.*, vol. 12, p. 587396, Nov. 10 2020. DOI: 10.3389/fnagi.2020.587396

[5] C. H. Hawkes, K. Del Tredici, and H. Braak, "Parkinson's disease: A dual-hit hypothesis," *Neuropathol. Appl. Neurobiol.*, vol. 33, no. 6, pp. 599–614, Dec. 2007. DOI: 10.1111/j.1365-2990.2007.00874.x

[6] E. Tolosa, A. Garrido, S. W. Scholz, and W. Poewe, "Challenges in the diagnosis of Parkinson's disease," *Lancet Neurol.*, vol. 20, no. 5, pp. 385–397, May 2021. DOI: 10.1016/S1474-4422(21)00030-2

[7] H. Braak, K. Del Tredici, U. Rüb, R. A. de Vos, E. N. Jansen Steur, and E. Braak, "Staging of brain pathology related to sporadic Parkinson's disease," *Neurobiol. Aging*, vol. 24, no. 2, pp. 197–211, Mar-Apr 2003. DOI: 10.1016/S0197-4580(02)00065-9

[8] E. Tolosa, G. Wenning, and W. Poewe, "The diagnosis of Parkinson's disease," *Lancet Neurol.*, vol. 5, no. 1, pp. 75–86, Jan. 2006. DOI: 10.1016/S1474-4422(05)70285-4

[9] P. Brown, "Oscillatory nature of human basal ganglia activity: Relationship to the pathophysiology of Parkinson's disease," *Mov. Disord.*, vol. 18, no. 4, pp. 357–363, Apr. 2003. DOI: 10.1002/mds.10358

[10] W. D. Hutchison, J. O. Dostrovsky, J. R. Walters, R. Courtemanche, T. Boraud, J. Goldberg, et al., "Neuronal oscillations in the basal ganglia and movement disorders: Evidence from whole animal and human recordings," *J. Neurosci.*, vol. 24, no. 42, pp. 9240–9243, Oct. 20 2004. DOI: 10.1523/JNEUROSCI.3366-04.2004

[11] A. Schnitzler and J. Gross, "Normal and pathological oscillatory communication in the brain," *Nat. Rev. Neurosci.*, vol. 6, no. 4, pp. 285–296, Apr. 2005. DOI: 10.1038/nrn1650

[12] H. W. Berendse and C. J. Stam, "Stage-dependent patterns of disturbed neural synchrony in Parkinson's disease," *Parkinsonism Relat. Disord.*, vol. 13, Suppl. 3, pp. S440–S445, 2007. DOI: 10.1016/S1353-8020(08)70046-4

[13] B. Pollok, V. Krause, W. Martsch, C. Wach, A. Schnitzler, and M. Südmeyer, "Motor-cortical oscillations in early stages of Parkinson's disease," *J. Physiol.*, vol. 590, no. 13, pp. 3203–3212, Jul. 1 2012. DOI: 10.1113/jphysiol.2012.231316

[14] E. Stein and I. Bar-Gad, "Beta oscillations in the cortico-basal ganglia loop during parkinsonism," *Exp. Neurol.*, vol. 245, pp. 52–59, Jul. 2013. DOI: 10.1016/j.expneurol.2012.07.023

[15] A. Oswal, P. Brown, and V. Litvak, "Synchronized neural oscillations and the pathophysiology of Parkinson's disease," *Curr. Opin. Neurol.*, vol. 26, no. 6, pp. 662–670, Dec. 2013. DOI: 10.1097/WCO.0000000000000034

[16] A. Singh, R. C. Cole, A. I. Espinoza, D. Brown, J. F. Cavanagh, and N. S. Narayanan, "Frontal theta and beta oscillations during lower-limb movement in Parkinson's disease," *Clin. Neurophysiol.*, vol. 131, no. 3, pp. 694–702, Mar. 2020, doi: 10.1016/j.clinph.2019.12.399.

[17] P. Brown and C. D. Marsden, "Bradykinesia and impairment of EEG desynchronization in Parkinson's disease," *Mov. Disord.*, vol. 14, no. 3, pp. 423–429, May 1999. DOI: 10.1002/1531-8257(199905)14:3¡423::AID-MDS1006¿3.0.CO;2-V

[18] P. Silberstein, A. Pogosyan, A. A. Kühn, G. Hotton, S. Tisch, A. Kupsch, et al., "Cortico-cortical coupling in Parkinson's disease and its modulation by therapy," *Brain*, vol. 128, Pt 6, pp. 1277–1291, Jun. 2005. DOI: 10.1093/brain/awh480

[19] S. R. Cole, R. van der Meij, E. J. Peterson, C. de Hemptinne, P. A. Starr, and B. Voytek, "Nonsinusoidal beta oscillations reflect cortical pathophysiology in Parkinson's disease," *J. Neurosci.*, vol. 37, no. 18, pp. 4830–4840, May 3 2017. DOI: 10.1523/JNEUROSCI.2208-16.2017

[20] Z. D. Zhou, L. X. Yi, D. Q. Wang, T. M. Lim, and E. K. Tan, "Role of dopamine in the pathophysiology of Parkinson's disease," *Transl. Neurodegener.*, vol. 12, no. 1, p. 44, Sep. 18 2023. DOI: 10.1186/s40035-023-00378-6

[21] M. J. Armstrong and M. S. Okun, "Diagnosis and treatment of parkinson disease: A review," *JAMA*, vol. 323, no. 6, pp. 548–560, Feb. 11 2020. DOI: 10.1001/jama.2019.22360

[22] T. Mima and M. Hallett, "Corticomuscular coherence: A review," *J. Clin. Neurophysiol.*, vol. 16, no. 6, pp. 501–511, Nov. 1999. DOI: 10.1097/00004691-199911000-00002

[23] J. Liu, Y. Sheng, and H. Liu, "Corticomuscular coherence and its applications: A review," *Front. Hum. Neurosci.*, vol. 13, p. 100, Mar. 20 2019. DOI: 10.3389/fnhum.2019.00100

[24] P. L. Nunez, R. Srinivasan, A. F. Westdorp, R. S. Wijesinghe, D. M. Tucker, R. B. Silberstein, et al., "EEG coherency. I: Statistics, reference electrode, volume conduction, Laplacians, cortical imaging, and interpretation at multiple scales," *Electroencephalogr. Clin. Neurophysiol.*, vol. 103, no. 5, pp. 499–515, Nov. 1997. DOI: 10.1016/S0013-4694(97)00066-7

[25] J.-P. Lachaux, A. Lutz, D. Rudrauf, D. Cosmelli, M. Le Van Quyen, J. Martinerie, et al., "Estimating the time-course of coherence between single-trial brain signals: An introduction to wavelet coherence," *Neurophysiol. Clin.*, vol. 32, no. 3, pp. 157–174, Jun. 2002. DOI: 10.1016/S0987-7053(02)00301-5

[26] S. N. Baker, E. Olivier, and R. N. Lemon, "Coherent oscillations in monkey motor cortex and hand muscle emg show task-dependent modulation," Journal of Physiology, vol. 501, no. Pt 1, pp. 225–241, May 1997. DOI: 10.1111/j.1469-7793.1997.225bo.x

[27] B. A. Conway, D. M. Halliday, S. F. Farmer, U. Shahani, P. Maas, A. I. Weir, et al., "Synchronization between motor cortex and spinal motoneuronal pool during the performance of a maintained motor task in man," *J. Physiol.*, vol. 489, Pt 3, pp. 917–924, Dec. 15 1995. DOI: 10.1113/jphysiol.1995.sp021104

[28] S. F. Farmer, F. D. Bremner, D. M. Halliday, J. R. Rosenberg, and J. A. Stephens, "The frequency content of common synaptic inputs to motoneurones studied during voluntary isometric contraction in man," *J. Physiol.*, vol. 470, no. 1, pp. 127–155, Oct. 1993. DOI: 10.1113/jphysiol.1993.sp019851

[29] D. M. Halliday, B. A. Conway, S. F. Farmer, and J. R. Rosenberg, "Using electroencephalography to study functional coupling between cortical activity and electromyograms during voluntary contractions in humans," *Neurosci. Lett.*, vol. 241, no. 1, pp. 5–8, Jan. 23 1998. DOI: 10.1016/S0304-3940(97)00964-6

[30] S. Salenius and R. Hari, "Synchronous cortical oscillatory activity during motor action," *Curr. Opin. Neurobiol.*, vol. 13, no. 6, pp. 678–684, Dec. 2003. DOI: 10.1016/j.conb.2003.10.008

[31] A. Andrykiewicz, L. Patino, J. R. Naranjo, M. Witte, M.-C. Hepp-Reymond, and R. Kristeva, "Corticomuscular synchronization with small and large dynamic force output," *BMC Neurosci.*, vol. 8, no. 1, p. 101, Nov. 27 2007. DOI: 10.1186/1471-2202-8-101

[32] X. Xi, X. Wu, Y.-B. Zhao, J. Wang, W. Kong, and Z. Luo, "Corticomuscular functional network: An exploration of cortico-muscular coupling in hand movements," *J. Neural Eng.*, vol. 18, no. 4, p. 046084, Jun. 9 2021. DOI: 10.1088/1741-2552/ac0586

[33] M. Fauvet, D. Gasq, A. Chalard, J. Tisseyre, and D. Amarantini, "Temporal dynamics of corticomuscular coherence reflects alteration of the central mechanisms of neural motor control in post-stroke patients," *Front. Hum. Neurosci.*, vol. 15, p. 682080, Jul. 23 2021. DOI: 10.3389/fnhum.2021.682080

[34] L. Zhou, B. Wu, B. Qin, F. Gao, W. Li, H. Hu, et al., "Corticomuscular coherence of time–frequency and spatial characteristics under movement observation, movement execution, and movement imagery," *Cogn. Neurodyn.*, vol. •••, pp. 1–18, 2023.

[35] R. Kristeva, L. Patino, and W. Omlor, "Beta-range cortical motor spectral power and corticomuscular coherence as a mechanism for effective corticospinal interaction during steady-state motor output," *Neuroimage*, vol. 36, no. 3, pp. 785–792, Jul. 1 2007. DOI: 10.1016/j.neuroimage.2007.03.025

[36] I. Mendez-Balbuena, F. Huethe, J. Schulte-Mönting, R. Leonhart, E. Manjarrez, and R. Kristeva, "Corticomuscular coherence reflects interindividual differences in the state of the corticomuscular network during low-level static and dynamic forces," *Cereb. Cortex*, vol. 22, no. 3, pp. 628–638, Mar. 2012. DOI: 10.1093/cercor/bhr147

[37] M. A. Perez, J. Lundbye-Jensen, and J. B. Nielsen, "Changes in corticospinal drive to spinal motoneurones following visuo-motor skill learning in humans," *J. Physiol.*, vol. 573, Pt 3, pp. 843–855, Jun. 15 2006. DOI: 10.1113/jphysiol.2006.105361

[38] T. Yamaguchi, C. Svane, C. R. Forman, M. M. Beck, S. S. Geertsen, J. Lundbye-Jensen, et al., "Transcranial alternating current stimulation

of the primary motor cortex after skill acquisition improves motor memory retention in humans: A double-blinded sham-controlled study," *Cereb. Cortex Commun.*, vol. 1, no. 1,tgaa047, Aug. 6 2020. DOI: 10.1093/texcom/tgaa047

[39] A. N. Johnson and M. Shinohara, "Corticomuscular coherence with and without additional task in the elderly," *J. Appl. Physiol.*, vol. 112, no. 6, pp. 970–981, Mar. 2012. DOI: 10.1152/japplphysiol.01079.2011

[40] M. B. Bayram, V. Siemionow, and G. H. Yue, "Weakening of corticomuscular signal coupling during voluntary motor action in aging," *Journals of Gerontology Series A: Biomedical Sciences and Medical Sciences*, vol. 70, no. 8, pp. 1037–1043, Aug. 2015. DOI: 10.1093/gerona/glv014

[41] D. Kamp, V. Krause, M. Butz, A. Schnitzler, and B. Pollok, "Changes of cortico-muscular coherence: An early marker of healthy aging?" *Age (Dordr.)*, vol. 35, no. 1, pp. 49–58, Feb. 2013. DOI: 10.1007/s11357-011-9329-y

[42] M. E. Spedden, J. B. Nielsen, and S. S. Geertsen, "Oscillatory corticospinal activity during static contraction of ankle muscles is reduced in healthy old versus young adults," *Neural Plast.*, vol. 2018, no. 1, p. 3432649, Apr. 26 2018. DOI: 10.1155/2018/3432649

[43] T. Mima, K. Toma, B. Koshy, and M. Hallett, "Coherence between cortical and muscular activities after subcortical stroke," *Stroke*, vol. 32, no. 11, pp. 2597–2601, Nov. 2001. DOI: 10.1161/hs1101.098764

[44] Y. Fang, J. J. Daly, J. Sun, K. Hvorat, E. Fredrickson, S. Pundik, et al., "Functional corticomuscular connection during reaching is weakened following stroke," *Clin. Neurophysiol.*, vol. 120, no. 5, pp. 994–1002, May 2009. DOI: 10.1016/j.clinph.2009.02.173

[45] K. von Carlowitz-Ghori, Z. Bayraktaroglu, F. U. Hohlefeld, F. Losch, G. Curio, and V. V. Nikulin, "Corticomuscular coherence in acute and chronic stroke," *Clin. Neurophysiol.*, vol. 125, no. 6, pp. 1182–1191, Jun. 2014. DOI: 10.1016/j.clinph.2013.11.006

[46] P. Belardinelli, L. Laer, E. Ortiz, C. Braun, and A. Gharabaghi, "Plasticity of premotor cortico-muscular coherence in severely impaired stroke patients with hand paralysis," *Neuroimage Clin.*, vol. 14, pp. 726–733, Mar. 16 2017. DOI: 10.1016/j.nicl.2017.03.005

[47] R. Aikio, K. Laaksonen, V. Sairanen, E. Parkkonen, A. Abou Elseoud, J. Kujala, et al., "CMC is more than a measure of corticospinal tract integrity in acute stroke patients," *Neuroimage Clin.*, vol. 32, p. 102818, 2021. DOI: 10.1016/j.nicl.2021.102818

[48] M. Proudfoot, F. van Ede, A. Quinn, G. L. Colclough, J. Wuu, K. Talbot, et al., "Impaired corticomuscular and interhemispheric cortical beta oscillation coupling in amyotrophic lateral sclerosis," *Clin. Neurophysiol.*, vol. 129, no. 7, pp. 1479–1489, Jul. 2018. DOI: 10.1016/j.clinph.2018.03.019

[49] K. M. Fisher, B. Zaaimi, T. L. Williams, S. N. Baker, and M. R. Baker, "Beta-band intermuscular coherence: A novel biomarker of upper motor neuron dysfunction in motor neuron disease," *Brain*, vol. 135, Pt 9, pp. 2849–2864, Sep. 2012. DOI: 10.1093/brain/aws150

[50] M. Padalino, C. Scardino, G. Zito, A. Cancelli, C. Cottone, M. Bertoli, et al., "Effects on motor control of personalized neuromodulation against multiple sclerosis fatigue," *Brain Topogr.*, vol. 34, no. 3, pp. 363–372, May 2021. DOI: 10.1007/s10548-021-00820-w

[51] H. Park, J. S. Kim, S. H. Paek, B. S. Jeon, J. Y. Lee, and C. K. Chung, "Cortico-muscular coherence increases with tremor improvement after deep brain stimulation in Parkinson's disease," *Neuroreport*, vol. 20, no. 16, pp. 1444–1449, Oct. 28 2009. DOI: 10.1097/WNR.0b013e328331a51a

[52] D. Weiss, S. Breit, J. Hoppe, A.-K. Hauser, D. Freudenstein, R. Krüger, et al., "Subthalamic nucleus stimulation restores the efferent cortical drive to muscle in parallel to functional motor improvement," *Eur. J. Neurosci.*, vol. 35, no. 6, pp. 896–908, Mar. 2012. DOI: 10.1111/j.1460-9568.2012.08014.x

[53] N. Zokaei, A. J. Quinn, M. T. Hu, M. Husain, F. van Ede, and A. C. Nobre, "Reduced cortico-muscular beta coupling in Parkinson's disease predicts motor impairment," *Brain Commun.*, vol. 3, no. 3,fcab179, Aug. 23 2021. DOI: 10.1093/braincomms/fcab179

[54] B. A. Conway, D. M. Halliday, and J. R. Rosenberg, "Rhythmic cortical activity and its relation to the neurogenic components of normal and pathological tremors," *Prog. Brain Res.*, vol. 123, pp. 437–444, 1999. DOI: 10.1016/S0079-6123(08)62879-4

[55] B. Hellwig, S. Häussler, M. Lauk, B. Guschlbauer, B. Köster, R. Kristeva-Feige, et al., "Tremor-correlated cortical activity detected by electroencephalography," *Clin. Neurophysiol.*, vol. 111, no. 5, pp. 806–809, May 2000. DOI: 10.1016/S1388-2457(00)00248-0

[56] A. Schnitzler, L. Timmermann, and J. Gross, "Physiological and pathological oscillatory networks in the human motor system," *J. Physiol. Paris*, vol. 99, no. 1, pp. 3–7, Jan. 2006. DOI: 10.1016/j.jphysparis.2005.06.010

[57] J. N. Caviness, C. H. Adler, M. N. Sabbagh, D. J. Connor, J. L. Hernandez, and T. D. Lagerlund, "Abnormal corticomuscular coherence is associated with the small amplitude cortical myoclonus in Parkinson's disease," *Mov. Disord.*, vol. 18, no. 10, pp. 1157–1162, Oct. 2003. DOI: 10.1002/mds.10525

[58] J. N. Caviness, H. A. Shill, M. N. Sabbagh, V. G. Evidente, J. L. Hernandez, and C. H. Adler, "Corticomuscular coherence is increased in the small postural tremor of Parkinson's disease," *Mov. Disord.*, vol. 21, no. 4, pp. 492–499, Apr. 2006. DOI: 10.1002/mds.20743

[59] Y. Yang, J. P. A. Dewald, F. C. T. van der Helm, and A. C. Schouten, "Unveiling neural coupling within the sensorimotor system: Directionality and nonlinearity," *Eur. J. Neurosci.*, vol. 48, no. 7, pp. 2407–2415, Oct. 2018. DOI: 10.1111/ejn.13692

[60] G. B. Ermentrout, "n: m phase-locking of weakly coupled oscillators," *J. Math. Biol.*, vol. 12, no. 3, pp. 327–342, 1981. DOI: 10.1007/BF00276920

[61] J.-P. Lachaux, E. Rodriguez, J. Martinerie, and F. J. Varela, "Measuring phase synchrony in brain signals," *Hum. Brain Mapp.*, vol. 8, no. 4, pp. 194–208, 1999. DOI: 10.1002/(SICI)1097-0193(1999)8:4¡194::AID-HBM4¿3.0.CO;2-C

[62] A. Bandrivskyy, A. Bernjak, P. McClintock, and A. Stefanovska, "*Wavelet phase coherence analysis: application to skin temperature and blood flow*," Cardiovascular engineering: an international journal, vol. 4, pp. 89–93, 2004.

[63] M. J. Kamiński and K. J. Blinowska, "A new method of the description of the information flow in the brain structures," *Biol. Cybern.*, vol. 65, no. 3, pp. 203–210, 1991. DOI: 10.1007/BF00198091

[64] F. Artoni, C. Fanciullacci, F. Bertolucci, A. Panarese, S. Makeig, S. Micera, et al., "Unidirectional brain to muscle connectivity reveals motor cortex control of leg muscles during stereotyped walking," *Neuroimage*, vol. 159, pp. 403–416, Oct. 1 2017. DOI: 10.1016/j.neuroimage.2017.07.013

[65] L. A. Baccalá and K. Sameshima, "Partial directed coherence: A new concept in neural structure determination," *Biol. Cybern.*, vol. 84, no. 6, pp. 463–474, Jun. 2001. DOI: 10.1007/PL00007990

[66] V. Youssofzadeh, D. Zanotto, K. Wong-Lin, S. K. Agrawal, and G. Prasad, "Directed functional connectivity in fronto-centroparietal circuit correlates with motor adaptation in gait training," *IEEE Trans. Neural Syst. Rehabil. Eng.*, vol. 24, no. 11, pp. 1265–1275, Nov. 2016. DOI: 10.1109/TNSRE.2016.2551642

[67] F. He, S. A. Billings, H.-L. Wei, and P. G. Sarrigiannis, "A nonlinear causality measure in the frequency domain: Nonlinear partial directed coherence with applications to EEG," *J. Neurosci. Methods*, vol. 225, pp. 71–80, Mar. 30 2014. DOI: 10.1016/j.jneumeth.2014.01.013

[68] R. Vicente, M. Wibral, M. Lindner, and G. Pipa, "Transfer entropy–a model-free measure of effective connectivity for the neurosciences," *J. Comput. Neurosci.*, vol. 30, no. 1, pp. 45–67, Feb. 2011. DOI: 10.1007/s10827-010-0262-3

[69] H. Hinrichs, T. Noesselt, and H.-J. Heinze, "Directed information flow: A model free measure to analyze causal interactions in event related EEG-MEG-experiments," *Hum. Brain Mapp.*, vol. 29, no. 2, pp. 193–206, Feb. 2008. DOI: 10.1002/hbm.20382

[70] X. Chen, Y. Zhang, S. Cheng, and P. Xie, "Transfer spectral entropy and application to functional corticomuscular coupling," *IEEE Trans. Neural Syst. Rehabil. Eng.*, vol. 27, no. 5, pp. 1092–1102, May 2019. DOI: 10.1109/TNSRE.2019.2907148

[71] Z. Zhang, S. Sun, M. Yi, X. Wu, and Y. Ding, "MIC as an appropriate method to construct the brain functional network," *BioMed Res. Int.*, vol. 2015, no. 1, p. 825136, 2015. DOI: 10.1155/2015/825136

[72] T. Liang, Q. Zhang, X. Liu, C. Lou, X. Liu, and H. Wang, "Time-frequency maximal information coefficient method and its application to functional corticomuscular coupling," *IEEE Trans. Neural Syst. Rehabil. Eng.*, vol. 28, no. 11, pp. 2515–2524, Nov. 2020. DOI: 10.1109/TNSRE.2020.3028199

[73] K. J. Friston, L. Harrison, and W. Penny, "Dynamic causal modelling," *Neuroimage*, vol. 19, no. 4, pp. 1273–1302, Aug. 2003. DOI: 10.1016/S1053-8119(03)00202-7

[74] V. N. Smelyanskiy, D. G. Luchinsky, A. Stefanovska, and P. V. McClintock, "Inference of a nonlinear stochastic model of the cardiorespiratory interaction," *Phys. Rev. Lett.*, vol. 94, no. 9, p. 098101, Mar. 11 2005. DOI: 10.1103/PhysRevLett.94.098101

[75] T. Stankovski, A. Duggento, P. V. McClintock, and A. Stefanovska, "Inference of time-evolving coupled dynamical systems in the presence of noise," *Phys. Rev. Lett.*, vol. 109, no. 2, p. 024101, Jul. 13 2012. DOI: 10.1103/PhysRevLett.109.024101

[76] T. Stankovski, A. Duggento, P. V. E. McClintock, and A. Stefanovska, "A tutorial on time-evolving dynamical bayesian inference," *Eur. Phys. J. Spec. Top.*, vol. 223, no. 13, pp. 2685–2703, 2014. DOI: 10.1140/epjst/e2014-02286-7

[77] P. Sauseng and W. Klimesch, "What does phase information of oscillatory brain activity tell us about cognitive processes?" *Neurosci. Biobehav. Rev.*, vol. 32, no. 5, pp. 1001–1013, Jul. 2008. DOI: 10.1016/j.neubiorev.2008.03.014

[78] S. J. K. Barnes, J. Bjerkan, P. T. Clemson, J. Newman, and A. Stefanovska, "Phase coherence-A time-localized approach to studying interactions," *Chaos*, vol. 34, no. 7, p. 073155, Jul. 1 2024. DOI: 10.1063/5.0202865

[79] A. K. Engel, P. Fries, and W. Singer, "Dynamic predictions: Oscillations and synchrony in top-down processing," *Nat. Rev. Neurosci.*, vol. 2, no. 10, pp. 704–716, Oct. 2001. DOI: 10.1038/35094565

[80] T. Womelsdorf and P. Fries, "Neuronal coherence during selective attentional processing and sensory-motor integration," *J. Physiol. Paris*, vol. 100, no. 4, pp. 182–193, Oct. 2006. DOI: 10.1016/j.jphysparis.2007.01.005

[81] A. Tomassini, E. Maris, P. Hilt, L. Fadiga, and A. D'Ausilio, "Visual detection is locked to the internal dynamics of cortico-motor control," *PLoS Biol.*, vol. 18, no. 10, p. e3000898, Oct. 20 2020. DOI: 10.1371/journal.pbio.3000898

[82] E. Maris, P. Fries, and F. van Ede, "Diverse phase relations among neuronal rhythms and their potential function," *Trends Neurosci.*, vol. 39, no. 2, pp. 86–99, Feb. 2016. DOI: 10.1016/j.tins.2015.12.004

[83] T. Mima, J. Steger, A. E. Schulman, C. Gerloff, and M. Hallett, "Electroencephalographic measurement of motor cortex control of muscle activity in humans," *Clin. Neurophysiol.*, vol. 111, no. 2, pp. 326–337, Feb. 2000. DOI: 10.1016/S1388-2457(99)00229-1

[84] J. Raethjen, M. Lindemann, M. Dümpelmann, R. Wenzelburger, H. Stolze, G. Pfister, et al., "Corticomuscular coherence in the 6-15 Hz band: Is the cortex involved in the generation of physiologic tremor?" *Exp. Brain Res.*, vol. 142, no. 1, pp. 32–40, Jan. 2002. DOI: 10.1007/s00221-001-0914-7

[85] S. Mehrkanoon, M. Breakspear, and T. W. Boonstra, "The reorganization of corticomuscular coherence during a transition between sensorimotor states," *Neuroimage*, vol. 100, pp. 692–702, Oct. 15 2014. DOI: 10.1016/j.neuroimage.2014.06.050

[86] Y. Yang, T. Solis-Escalante, J. Yao, A. Daffertshofer, A. C. Schouten, and F. C. van der Helm, "A general approach for quantifying nonlinear connectivity in the nervous system based on phase coupling," *Int. J. Neural Syst.*, vol. 26, no. 1, p. 1550031, Feb. 2016. DOI: 10.1142/S0129065715500318

[87] N. Parmar, P. Sirpal, W. A. Sikora, J. P. Dewald, H. H. Refai, and Y. Yang, "Beta-band cortico-muscular phase coherence in hemiparetic stroke," *Biomed. Signal Process. Control*, vol. 97, p. 106719, 2024. DOI: 10.1016/j.bspc.2024.106719

[88] Y. Kuramoto, "Self-entrainment of a population of coupled nonlinear oscillators," in *International symposium on mathematical problems in theoretical physics*. Springer, 1975, pp. 420–422. DOI: 10.1007/BFb0013365

[89] J. A. Acebrón, L. L. Bonilla, C. J. P. Vicente, F. Ritort, and R. Spigler, "The kuramoto model: A simple paradigm for synchronization phenomena," *Rev. Mod. Phys.*, vol. 77, no. 1, pp. 137–185, 2005. DOI: 10.1103/RevModPhys.77.137

[90] K. J. Friston, "Functional and effective connectivity: A review," *Brain Connect.*, vol. 1, no. 1, pp. 13–36, 2011. DOI: 10.1089/brain.2011.0008

[91] T. Stankovski, V. Ticcinelli, P. V. E. McClintock, and A. Stefanovska, "Neural cross-frequency coupling functions," *Front. Syst. Neurosci.*, vol. 11, p. 33, Jun. 15 2017. DOI: 10.3389/fnsys.2017.00033

[92] T. Stankovski, T. Pereira, P. V. McClintock, and A. Stefanovska, "Coupling functions: Universal insights into dynamical interaction mechanisms," *Rev. Mod. Phys.*, vol. 89, no. 4, p. 045001, 2017. DOI: 10.1103/RevModPhys.89.045001

[93] Z. Šverko, J. Sajovic, G. Drevenšek, S. Vlahinić, and P. Rogelj, "Generation of oscillatory synthetic signal simulating brain network dynamics," 2021 44th International Convention on Information, Communication and Electronic Technology, MIPRO 2021 - Proceedings, pp. 141–146, 2021. DOI: 10.23919/MIPRO52101.2021.9597039

[94] D. Manasova and T. Stankovski, "Neural cross-frequency coupling functions in sleep," *Neuroscience*, vol. 523, pp. 20–30, Jul. 15 2023. DOI: 10.1016/j.neuroscience.2023.05.016

[95] D. Lukarski, S. Petkoski, P. Ji, and T. Stankovski, "Delta-alpha cross-frequency coupling for different brain regions," *Chaos*, vol. 33, no. 10, p. 103126, Oct. 1 2023. DOI: 10.1063/5.0157979

[96] C. G. Goetz, B. C. Tilley, S. R. Shaftman, G. T. Stebbins, S. Fahn, P. Martinez-Martin, et al.; Movement Disorder Society UPDRS Revision Task Force, "Movement Disorder Society-sponsored revision of the Unified Parkinson's Disease Rating Scale (MDS-UPDRS): Scale presentation and clinimetric testing results," *Mov. Disord.*, vol. 23, no. 15, pp. 2129–2170, Nov. 15 2008. DOI: 10.1002/mds.22340

[97] U. Marusic, M. Peskar, M. M. Šömen, M. Kalc, A. Holobar, K. Gramann, et al., *Neuromuscular assessment of force development, postural, and gait performance under cognitive-motor dual-tasking in healthy older adults and people with early Parkinson's disease: Study protocol for a cross-sectional Mobile Brain/Body Imaging (MoBI) study*, vol. 3. Open Research Europe, 2023.

[98] R. Oostenveld and P. Praamstra, "The five percent electrode system for high-resolution EEG and ERP measurements," *Clin. Neurophysiol.*, vol. 112, no. 4, pp. 713–719, Apr. 2001. DOI: 10.1016/S1388-2457(00)00527-7

[99] A. Delorme and S. Makeig, "EEGLAB: An open source toolbox for analysis of single-trial EEG dynamics including independent component analysis," *J. Neurosci. Methods*, vol. 134, no. 1, pp. 9–21, Mar. 15 2004. DOI: 10.1016/j.jneumeth.2003.10.009

[100] J. Newman, G. Lancaster, and A. Stefanovska, Multiscale Oscillatory Dynamics Analysis v1.01: User Manual, September 2018. [Online]. Available: `https://www.matrix-inst.org.au/wp_Matrix2016/wp-content/uploads/2019/2019_07_Angelova/MODA-User-Manual.pdf`

[101] A. de Cheveigné, "ZapLine: A simple and effective method to remove power line artifacts," *Neuroimage*, vol. 207, p. 116356, Feb. 15 2020. DOI: 10.1016/j.neuroimage.2019.116356

[102] M. Klug and N. A. Kloosterman, "Zapline-plus: A Zapline extension for automatic and adaptive removal of frequency-specific noise artifacts in M/EEG," *Hum. Brain Mapp.*, vol. 43, no. 9, pp. 2743–2758, Jun. 15 2022. DOI: 10.1002/hbm.25832

[103] L. Pion-Tonachini, K. Kreutz-Delgado, and S. Makeig, "ICLabel: An automated electroencephalographic independent component classifier, dataset, and website," *Neuroimage*, vol. 198, pp. 181–197, Sep. 2019. DOI: 10.1016/j.neuroimage.2019.05.026

[104] R. Oostenveld, P. Praamstra, D. F. Stegeman, and A. van Oosterom, "Overlap of attention and movement-related activity in lateralized event-related brain potentials," *Clin. Neurophysiol.*, vol. 112, no. 3, pp. 477–484, Mar. 2001. DOI: 10.1016/S1388-2457(01)00460-6

[105] J. Bigot, M. Longcamp, F. Dal Maso, and D. Amarantini, "A new statistical test based on the wavelet cross-spectrum to detect time-frequency dependence between non-stationary signals: Application to the analysis of cortico-muscular interactions," *Neuroimage*, vol. 55, no. 4, pp. 1504–1518, Apr. 15 2011. DOI: 10.1016/j.neuroimage.2011.01.033

[106] V. M. McClelland, Z. Cvetkovic, and K. R. Mills, "Rectification of the EMG is an unnecessary and inappropriate step in the calculation of Corticomuscular coherence," *J. Neurosci. Methods*, vol. 205, no. 1, pp. 190–201, Mar. 30 2012. DOI: 10.1016/j.jneumeth.2011.11.001

[107] Y. Ruiz-Gonzalez, L. Velázquez-Pérez, R. Rodríguez-Labrada, R. Torres-Vega, and U. Ziemann, "Role of emg rectification for corticomuscular and intermuscular coherence estimation of spinocerebellar ataxia type 2 (sca2)," in Progress in Pattern Recognition, Image Analysis, Computer Vision, and Applications: *24th Iberoamerican Congress, CIARP 2019*, Havana, Cuba, October 28-31, 2019, Proceedings 24. Springer, 2019, pp. 306–315. DOI: 10.1007/978-3-030-33904-3_28

[108] W. Penfield and E. Boldrey, "Somatic motor and sensory representation in the cerebral cortex of man as studied by electrical stimulation," *Brain*, vol. 60, no. 4, pp. 389–443, 1937. DOI: 10.1093/brain/60.4.389

[109] C. J. Scheirer, W. S. Ray, and N. Hare, "The analysis of ranked data derived from completely randomized factorial designs," *Biometrics*, vol. 32, no. 2, pp. 429–434, Jun. 1976. DOI: 10.2307/2529511

[110] Y. Benjamini and Y. Hochberg, "Controlling the false discovery rate: A practical and powerful approach to multiple testing," *J. R. Stat. Soc. Series B Stat. Methodol.*, vol. 57, no. 1, pp. 289–300, 1995. DOI: 10.1111/j.2517-6161.1995.tb02031.x

[111] F. Mormann, K. Lehnertz, P. David, and C. E. Elger, "Mean phase coherence as a measure for phase synchronization and its application to the eeg of epilepsy patients," *Physica D*, vol. 144, no. 3-4, pp. 358–369, 2000. DOI: 10.1016/S0167-2789(00)00087-7

[112] F. Wilcoxon, *"Individual comparisons by ranking methods," in Breakthroughs in statistics: Methodology and distribution*. Springer, 1992, pp. 196–202. DOI: 10.1007/978-1-4612-4380-9_16

[113] G. Lancaster, D. Iatsenko, A. Pidde, V. Ticcinelli, and A. Stefanovska, "Surrogate data for hypothesis testing of physical systems," *Phys. Rep.*, vol. 748, pp. 1–60, 2018. DOI: 10.1016/j.physrep.2018.06.001

[114] B. Kralemann, L. Cimponeriu, M. Rosenblum, A. Pikovsky, and R. Mrowka, "Phase dynamics of coupled oscillators reconstructed from data," *Phys. Rev. E Stat. Nonlin. Soft Matter Phys.*, vol. 77, 6 Pt 2, p. 066205, Jun. 2008. DOI: 10.1103/PhysRevE.77.066205

[115] B. Kralemann, M. Frühwirth, A. Pikovsky, M. Rosenblum, T. Kenner, J. Schaefer, et al., "In vivo cardiac phase response curve elucidates human respiratory heart rate variability," *Nat. Commun.*, vol. 4, no. 1, p. 2418, 2013. DOI: 10.1038/ncomms3418

[116] J. H. Zar, "*Spearman rank correlation*," Encyclopedia of Biostatistics, vol. 7, 2005. DOI: 10.1002/0470011815.b2a15150

[117] R. Matsuya, J. Ushiyama, and J. Ushiba, "Inhibitory interneuron circuits at cortical and spinal levels are associated with individual differences in corticomuscular coherence during isometric voluntary contraction," *Sci. Rep.*, vol. 7, no. 1, p. 44417, Mar. 14 2017. DOI: 10.1038/srep44417

[118] R. G. Abeysuriya, J. Hadida, S. N. Sotiropoulos, S. Jbabdi, R. Becker, B. A. E. Hunt, M. J. Brookes, and M. W. Woolrich, "A biophysical model of dynamic balancing of excitation and inhibition in fast oscillatory large-scale networks," *PLoS Computational Biology*, vol. 14, no. 2, pp. e1006007, 2018.

[119] F. A. Torres, M. Otero, C. A. Lea-Carnall, J. Cabral, A. Weinstein, and W. El-Deredy, "Emergence of multiple spontaneous coherent subnetworks from a single configuration of human connectome-coupled oscillators model," *bioRxiv*, pp. 2024–01, 2024.

[120] D. Kudo, T. Koseki, N. Katagiri, K. Yoshida, K. Takano, M. Jin, et al., "Individualized beta-band oscillatory transcranial direct current stimulation over the primary motor cortex enhances corticomuscular coherence and corticospinal excitability in healthy individuals," *Brain Stimul.*, vol. 15, no. 1, pp. 46–52, Jan-Feb 2022. DOI: 10.1016/j.brs.2021.11.004

[121] J. Prado, R. Mutreja, H. Zhang, R. Mehta, A. S. Desroches, J. E. Minas, et al., "Distinct representations of subtraction and multiplication in the neural systems for numerosity and language," *Hum. Brain Mapp.*, vol. 32, no. 11, pp. 1932–1947, Nov. 2011. DOI: 10.1002/hbm.21159

[122] *H. Pashler, The Psychology of Attention*. Cambridge, MA: MIT Press, 1998.

[123] I. Koch, E. Poljac, H. Müller, and A. Kiesel, "Cognitive structure, flexibility, and plasticity in human multitasking-An integrative review of dual-task and task-switching research," *Psychol. Bull.*, vol. 144, no. 6, pp. 557–583, Jun. 2018. DOI: 10.1037/bul0000144

[124] S. T. Christie and P. Schrater, "Cognitive cost as dynamic allocation of energetic resources," *Front. Neurosci.*, vol. 9, p. 289, Aug. 24 2015. DOI: 10.3389/fnins.2015.00289

[125] B. Hommel, "Dual-task performance: Theoretical analysis and an event-coding account," *J. Cogn.*, vol. 3, no. 1, p. 29, Sep. 29 2020. DOI: 10.5334/joc.114

[126] J. Volkmann, M. Joliot, A. Mogilner, A. A. Ioannides, F. Lado, E. Fazzini, et al., "Central motor loop oscillations in parkinsonian resting tremor revealed by magnetoencephalography," *Neurology*, vol. 46, no. 5, pp. 1359–1370, May 1996. DOI: 10.1212/WNL.46.5.1359

[127] P. C. Poortvliet, K. J. Tucker, S. Finnigan, D. Scott, P. Sowman, and P. W. Hodges, "Cortical activity differs between position- and force-control knee extension tasks," *Exp. Brain Res.*, vol. 233, no. 12, pp. 3447–3457, Dec. 2015. DOI: 10.1007/s00221-015-4404-8

[128] J. T. Gwin and D. P. Ferris, "Beta- and gamma-range human lower limb corticomuscular coherence," *Front. Hum. Neurosci.*, vol. 6, p. 258, Sep. 11 2012. DOI: 10.3389/fnhum.2012.00258

[129] E. Heinrichs-Graham, T. W. Wilson, P. M. Santamaria, S. K. Heithoff, D. Torres-Russotto, J. A. Hutter-Saunders, et al., "Neuromagnetic evidence of abnormal movement-related beta desynchronization in Parkinson's disease," *Cereb. Cortex*, vol. 24, no. 10, pp. 2669–2678, Oct. 2014. DOI: 10.1093/cercor/bht121

[130] L. Roeder, T. W. Boonstra, and G. K. Kerr, "Corticomuscular control of walking in older people and people with Parkinson's disease," *Sci. Rep.*, vol. 10, no. 1, p. 2980, Feb. 19 2020. DOI: 10.1038/s41598-020-59810-w

[131] O. Beauchet, V. Dubost, K. Aminian, R. Gonthier, and R. W. Kressig, "Dual-task-related gait changes in the elderly: Does the type of cognitive task matter?" *J. Mot. Behav.*, vol. 37, no. 4, pp. 259–264, Jul. 2005.

[132] C. Voelcker-Rehage and J. L. Alberts, "Effect of motor practice on dual-task performance in older adults," *J. Gerontol. B Psychol. Sci. Soc. Sci.*, vol. 62, no. 3, pp. 141–148, May 2007. DOI: 10.1093/geronb/62.3.P141

[133] R. Kristeva-Feige, C. Fritsch, J. Timmer, and C.-H. Lücking, "Effects of attention and precision of exerted force on beta range EEG-EMG synchronization during a maintained motor contraction task," *Clin. Neurophysiol.*, vol. 113, no. 1, pp. 124–131, Jan. 2002. DOI: 10.1016/S1388-2457(01)00722-2

[134] A. N. Johnson, L. A. Wheaton, and M. Shinohara, "Attenuation of corticomuscular coherence with additional motor or non-motor task," *Clin. Neurophysiol.*, vol. 122, no. 2, pp. 356–363, Feb. 2011. DOI: 10.1016/j.clinph.2010.06.021

[135] F. Negro and D. Farina, "Linear transmission of cortical oscillations to the neural drive to muscles is mediated by common projections to populations of motoneurons in humans," *J. Physiol.*, vol. 589, Pt 3, pp. 629–637, Feb. 1 2011. DOI: 10.1113/jphysiol.2010.202473

[136] E. R. Williams and S. N. Baker, "Circuits generating corticomuscular coherence investigated using a biophysically based computational model. I. Descending systems," *J. Neurophysiol.*, vol. 101, no. 1, pp. 31–41, Jan. 2009. DOI: 10.1152/jn.90362.2008

[137] T. W. Boonstra, B. C. van Wijk, P. Praamstra, and A. Daffertshofer, "Corticomuscular and bilateral EMG coherence reflect distinct aspects of neural synchronization," *Neurosci. Lett.*, vol. 463, no. 1, pp. 17–21, Sep. 29 2009. DOI: 10.1016/j.neulet.2009.07.043

[138] T. W. Boonstra, The potential of corticomuscular and intermuscular coherence for research on human motor control. 2013, p. 855.

[139] T. D. Aumann and Y. Prut, "Do sensorimotor beta-oscillations maintain muscle synergy representations in primary motor cortex?" *Trends Neurosci.*, vol. 38, no. 2, pp. 77–85, Feb. 2015. DOI: 10.1016/j.tins.2014.12.002

[140] A. Reyes, C. M. Laine, J. J. Kutch, and F. J. Valero-Cuevas, "Beta-band corticomuscular drive reflects muscle coordination strategies," *Front. Comput. Neurosci.*, vol. 11, p. 17, Apr. 4 2017. DOI: 10.3389/fncom.2017.00017

[141] C. S. Zandvoort, J. H. van Dieën, N. Dominici, and A. Daffertshofer, "The human sensorimotor cortex fosters muscle synergies through cortico-synergy coherence," *Neuroimage*, vol. 199, pp. 30–37, Oct. 1 2019. DOI: 10.1016/j.neuroimage.2019.05.041

[142] J. Liu, G. Tan, J. Wang, Y. Wei, Y. Sheng, H. Chang, et al., "Closed-loop construction and analysis of cortico-muscular-cortical functional network after stroke," *IEEE Trans. Med. Imaging*, vol. 41, no. 6, pp. 1575–1586, Jun. 2022. DOI: 10.1109/TMI.2022.3143133

[143] T. Stankovski, V. Ticcinelli, P. V. McClintock, and A. Stefanovska, "Coupling functions in networks of oscillators," *New J. Phys.*, vol. 17, no. 3, p. 035002, 2015. DOI: 10.1088/1367-2630/17/3/035002

[144] J. Ushiyama, T. Suzuki, Y. Masakado, K. Hase, A. Kimura, M. Liu, et al., "Between-subject variance in the magnitude of corticomuscular coherence during tonic isometric contraction of the tibialis anterior muscle in healthy young adults," *J. Neurophysiol.*, vol. 106, no. 3, pp. 1379–1388, Sep. 2011. DOI: 10.1152/jn.00193.2011